

1 ***Fifty-six years of Surface Solar Radiation and Sunshine***
2 ***Duration over São Paulo, Brazil: 1961 - 2016***

3

4 ***Marcia Akemi Yamasoe^{1,3}, Nilton Manuel Évora do Rosário²,***
5 ***Samantha Novaes Santos Martins Almeida³, Martin Wild⁴***

Formatado: Português (Brasil)

6 [1] Departamento de Ciências Atmosféricas, Instituto de Astronomia, Geofísica e
7 Ciências Atmosféricas, Universidade de São Paulo, São Paulo, Brazil

8 [2] Departamento de Ciências Ambientais, Universidade Federal de São Paulo,
9 Diadema, São Paulo, Brazil

10 [3] Seção de Serviços Meteorológicos do Instituto de Astronomia, Geofísica e Ciências
11 Atmosféricas, Universidade de São Paulo, São Paulo, Brazil

12 [4] Institute for Atmospheric and Climate Science, ETH Zurich, Switzerland

13

14 Correspondence to: M. A. Yamasoe (marcia.yamasoe@iag.usp.br)

15

16
17
18
19
20
21
22
23
24
25
26
27
28
29
30
31
32
33
34
35
36
37
38
39
40

Abstract

Fifty-six years (1961 – 2016) of daily surface downward solar irradiation, sunshine duration, diurnal temperature range and the fraction of the sky covered by clouds in the city of São Paulo, Brazil, were analysed. The main purpose was to contribute to the characterization and understanding of the dimming and brightening effects on solar global radiation in this part of South America. As observed in most of the previous studies worldwide, in this study, during the period between 1961 ~~up to~~ ~~the~~ ~~and~~ early 1980's, ~~more specifically up to 1983,~~ a negative trend ~~of about -0.40 kJm^{-2}~~ ~~per decade, with a significance level of $p = 0.101$~~ in surface solar irradiation ~~of~~ was detected in São Paulo, characterizing the occurrence of a dimming effect. Sunshine duration and the diurnal temperature range also presented negative trends, in opposition to the positive trend observed in the cloud cover fraction ~~A similar behaviour, a negative trend, was also observed for sunshine duration and the diurnal temperature range, the three variables in opposition to the trend in the cloud cover fraction of 2.9 % per decade ($p = 0.013$).~~ However, a brightening effect, as observed in western industrialized countries in more recent years, was not observed. Instead, for surface downward irradiation, the negative trend persisted, with a trend of -0.13 kJm^{-2} per decade, with a p-value of 0.006, for the 56 years of data, and in consonance to the cloud cover fraction increasing trend, but not statistically significant, of 0.3 % per decade (p -value = 0.198). The trends for sunshine duration and the diurnal temperature range, by contrast, changed signal, as confirmed by a piecewise linear regression model ~~Instead, for surface downward irradiation, the negative trend persisted, with a trend of -0.39 kJm^{-2} per decade ($p = 0.003$) and in consonance to the cloud cover fraction increasing trend of 0.8 % per decade ($p = 0.075$). The trends for sunshine duration and the diurnal~~

Formatado: Não Realce

Formatado: Não Realce

Formatado: Não Realce

Formatado: Não Realce

Formatado: Não Realce

Formatado: Não Realce

Formatado: Não Realce

Formatado: Não Realce

Formatado: Não Realce

41 ~~temperature range, by contrast, changed signal.~~ Some possible causes for the
42 discrepancy ~~we~~are discussed, such as the frequency of fog occurrence, urban heat island
43 effects, horizontal visibility (as a proxy for aerosol loading variability) and greenhouse
44 gas concentration increase. Future studies on the aerosol effect are planned, particularly
45 with higher temporal resolution as well as modelling studies, to better analyse the
46 contribution of each possible causes.

47

48 **1 Introduction**

49 Ultimately, the downward solar radiation at the surface is the main source of
50 energy that drives Earth's biological, chemical, and physical processes (Wild et al.,
51 2013, Kren et al., 2017), from local to global scales. Therefore, the assessment of the
52 variability of the downward solar radiation at the surface is a key step in the efforts to
53 understand Earth's climate system variability. Before reaching the surface, solar
54 radiation can be attenuated mainly by aerosols and clouds, through scattering and
55 absorption processes, and to a lesser extent, through Rayleigh scattering by atmospheric
56 gases, absorption by ozone and water vapor, for example. In this context, during the last
57 half-century, long term changes in the amount of surface solar radiation have been
58 investigated worldwide (Dutton et al., 1991, Stanhill and Cohen 2001, Wild et al. 2005,
59 Shi et al., 2008, Wild, 2009, 2012, Ohvri, et al., 2009). At least two trends have been
60 well established and documented over wide regions of the world, a decline in surface
61 solar radiation between 1950s and 1980s, named "Global Dimming" and an increase,
62 from 1980s to 2000s, termed "Brightening" (Stanhill and Cohen, 2001; Wild, 2009,
63 2012).

64 The global dimming definition, according to Stanhill and Cohen (2001), refers to
65 a widespread and significant reduction in global irradiance, that is the flux of solar

66 radiation reaching the earth's surface comprising the direct solar beam and the diffuse
67 radiation scattered by the sky and clouds. However, among these studies, while the
68 dimming phase has been a consensus for all locations analysed, the brightening phase
69 was not (Zerefos et al., 2009, Wild, 2012). Over India, for example, the dimming phase
70 seems to last throughout the 2000s (Kumari and Goswami, 2010). The continuous
71 dimming in India and the renewed dimming in China from 2000s, opposing to a
72 persistent brightening over Europe and the United States, have been linked to trends in
73 atmospheric anthropogenic aerosol loadings (Wild, 2012). By contrast, other studies
74 suggested that changes in cloud cover rather than anthropogenic aerosol emissions
75 played a major role in determining solar dimming and brightening during the last half
76 century (Stanhill et al., 2014). Therefore, the drivers of dimming and brightening are a
77 matter of ongoing research and debate (Manara et al., 2016, Kazadzis et al., 2018,
78 Manara et al., 2019, Yang et al. 2019). The role of these trends in the masking of
79 temperature increases due to increasing greenhouse gases (GHG) concentration has
80 been discussed (Wild et al., 2007). Furthermore, a comprehensive assessment of the
81 spatial scale of both dimming and brightening is critical for a conclusive analysis of the
82 likely drivers and implications for the current global climate variability. Large portions
83 of the globe are still lacking any evaluation on this matter, such as Africa (Wild, 2009),
84 which is a challenge for the spatial characterization of both dimming and brightening
85 trends.

86 Among the rare studies focusing on the South American subcontinent, Raichijk
87 (2012) discussed the trends over South America, analysing sunshine duration (SD) data
88 from 1961 to 2004. The author divided South America in five climatic regions. In three
89 of them, also the one where the city of São Paulo is located, statistically significant
90 negative trends were observed on an annual basis, from 1961 up to 1990. From 1991 to

91 2004 a positive trend was observed in four of the five regions with a significance level
92 higher than 90%.

93 The alternative use of SD is mainly due to the lack of a consistent long-term
94 network for the monitoring of surface solar radiation across the continent, therefore
95 alternative proxies have to be found in order to provide an estimate of surface solar
96 radiation long term trends. Another variable commonly used to investigate surface solar
97 radiation trends is the diurnal temperature range (DTR), the difference between daily
98 maximum (T_{\max}) and minimum (T_{\min}) air temperature measured near the surface
99 (Bristow and Campbell, 1984, Wild et al. 2007, Makowski et al. 2008).

100 The present study takes advantage of fifty-six years of a unique high quality
101 concurrent records of surface solar irradiation (SSR), sunshine duration (SD), diurnal
102 temperature range (DTR) and cloud cover fraction (CCF), i.e., the fraction of the sky
103 covered by clouds, from 1961 to 2016, in the city of São Paulo, Brazil, to provide a
104 perspective on dimming and brightening trends with an extended database.

105 Two questions are addressed in this study: 1) How was the decadal variability of
106 SSR over the 56 years of data?; 2) Can SD and DTR be adopted as proxies to infer SSR
107 variability in São Paulo? To answer to these questions, we organize the manuscript as
108 follows: in section 2 we present the data and methods of analysis; section 3 is divided in
109 3 parts. In the first part of that section, we discuss the annual trends in SSR, SD and
110 DTR; in the second, we focus the analysis on horizontal visibility and the number of
111 foggy days; and, in the third part of section 3, we discuss the trends in the maximum
112 and minimum air temperatures near the surface. Section 4 summarizes the main
113 conclusions and discusses possible future work on the subject.

114

115 **2 Observational Data and Methods**

116 The long-term measurements used in this study were collected at the
117 meteorological station operated by the Instituto de Astronomia, Geofísica e Ciências
118 Atmosféricas from the Universidade de São Paulo (IAG/USP), located at latitude
119 23.65° S and longitude 46.62° W, 799 m above sea level. Figure 1 shows the
120 geographical location of the meteorological station. The site is surrounded by a
121 vegetated area due to its location inside a park.

122



123

124 Figure 1 – São Paulo state and a zooming in view of São Paulo Metropolitan Area and
125 the location of the meteorological station of Instituto de Astronomia, Geofísica e
126 Ciências Atmosféricas from Universidade de São Paulo (EM-IAG). Adapted from ©
127 Google Earth (US Dept. of State Geographer – Data SIO, NOAA, U. S. Navy, NGA,
128 GEBCO - Image Landsat/Copernicus).

129

130 The downward solar irradiation has been measured since 1961 using an
131 Actinograph Robitzsch-Fuess model 58d, with 5% instrumental uncertainty (Plana-
132 Fattori and Ceballos, 1988). The long-term variation of the sensor calibration of -
133 1.5 % per decade was taken into account. This trend was estimated by comparing one
134 year of data collected in parallel and at the same site with a brand new Actinograph
135 Robitzsch-Fuess model 58dc, in 2014 and agrees with previous estimations performed
136 by Plana-Fattori and Ceballos (1988) (See supplementary information for details of the

137 comparison). Sunshine duration data was collected with a Campbell-Stokes sunshine
138 recorder (Horseman et al., 2008) from 1933 to the present, while daily maximum and
139 minimum air temperatures ~~were monitored since~~~~started to be monitored in~~ 1935. Daily
140 maximum and minimum temperatures were used to estimate the diurnal temperature
141 range as it is simply the difference between the maximum and minimum daily
142 temperatures. Diurnal cloud cover fraction was determined from visual inspection made
143 every hour from 7:00 AM to 6:00 PM (local time) (Yamasoe et al. 2017).

Formatado: Não Realce

144 Annual mean values of downward solar irradiation data at the surface were used
145 to characterize dimming and brightening trends while sunshine duration and diurnal
146 temperature range measurements at the same site were used to provide independent
147 information.

148 In order to ~~detect possible temporal changes~~~~estimate trends~~, avoiding
149 autocorrelation in the data, the modified Mann-Kendall trend test proposed by Hamed
150 and Rao (1998) was applied to the variables, while the regression coefficient was
151 estimated based on Sen (1968). A statistically significant trend at the 95% confidence
152 level was detected if the absolute value of Z was above 1.96, ~~We also applied a~~
153 ~~piecewise linear regression model, proposed by Muggeo (2003) to detect any trend~~
154 ~~changes.~~

Formatado: Não Realce

155 According to the meteorological station records, completely cloud free days are
156 extremely rare in São Paulo, being more common from June to the beginning of
157 September, corresponding to the southern hemisphere wintertime, when dry conditions
158 prevail in the region (Yamasoe et al., 2017). The number of days without clouds per
159 year, from sunrise to sunset, varied from 1 to 23. This extremely low number of clear
160 sky days restricted the analysis in such conditions, mainly at aiming to evaluate the
161 exclusive role of aerosol variability in the long-term trends.

162 To complement the analysis and help interpreting the findings, we included data
163 about the occurrence of fog and horizontal visibility. The first information was analysed
164 in terms of the number of foggy days (NFD). If fog was observed on a given day, the
165 day received the number 1, otherwise, the number is 0. Horizontal visibility, or simply
166 visibility, is recorded every hour, from 7:00 A.M. till midnight, at the meteorological
167 station. Visibility can be affected by haze and fog conditions but is less sensitive to
168 cloud variability. Thus, all-sky visibility data was used as a proxy for aerosol loading
169 (Zhang et al., 2020). However, to avoid the effect of fog on the horizontal visibility, we
170 limited the data from 10:00 AM to 03:00 PM, as, at the location, fog is usually observed
171 either early in the morning or late in the afternoon, when low temperature and high
172 humidity scenarios are more likely to occur in São Paulo. Therefore, the reduction in
173 visibility from 10:00 AM to 03:00 PM is expected to be related to the atmospheric
174 turbidity. The impact of aerosol on SSR is higher from August to October, when
175 advection of smoke plumes from long range transports can reach São Paulo, summing
176 up to the typical increase in the local pollution associated with the dominance of low
177 dispersion scenarios during this time of the year (Yamasoe et al., 2017). This is also
178 when low temperatures and stable atmospheric conditions favour fog formation. Thus,
179 the analysis of both variables is limited to the months of July to October.

180 To verify if the effect of visibility on SSR and SD could be detected, data
181 measured on clear sky days were analysed normalizing SSR by the expected irradiation
182 at the top of the atmosphere (TSR), determining the solar transmittance and minimizing
183 the seasonal variability. Sunshine duration (SD or n) was normalized to the day-length
184 (N). Top of the atmosphere irradiation and the day-length were estimated using
185 formulas proposed by Paltridge and Platt (1976), which also include the variation of
186 Sun-Earth distance.

187

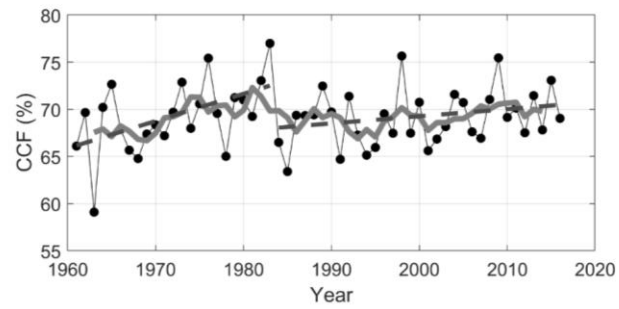
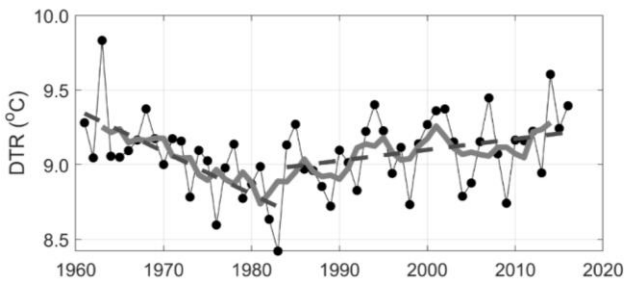
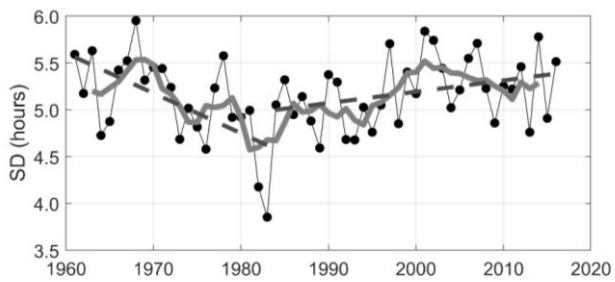
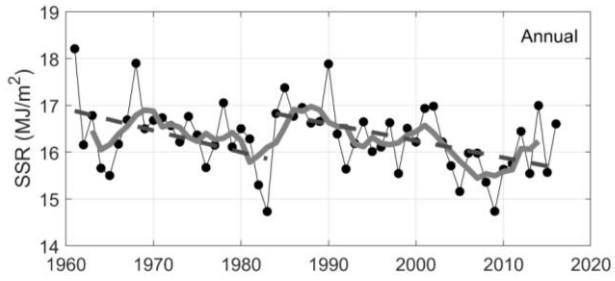
188 3 Results

189 3.1 SSR, SD, DTR and CCF annual mean variability and trends

190 Figure 2 illustrates the time series of the annual mean values for SSR, SD, DTR
191 and CCF, showing that all the analysed variables exhibited a large variability from year
192 to year. SSR, SD and DTR presented a decreasing trend up to the beginning of the
193 1980's, in opposition, therefore consistent, to the CCF trend. According to Rosas et al.
194 (2019), who analysed the same cloud fraction database from the meteorological station,
195 focusing on the climatology for different cloud types and base heights, all cloud types,
196 except for the middle level clouds, presented a positive trend, which is confirmed by
197 this study. ~~A statistically significant trend, at the 95 % level, was observed for stratiform
198 cloud fraction of 4.8 % per decade and for cirrus of 1.4 % per decade, from 1958 to
199 1986.~~

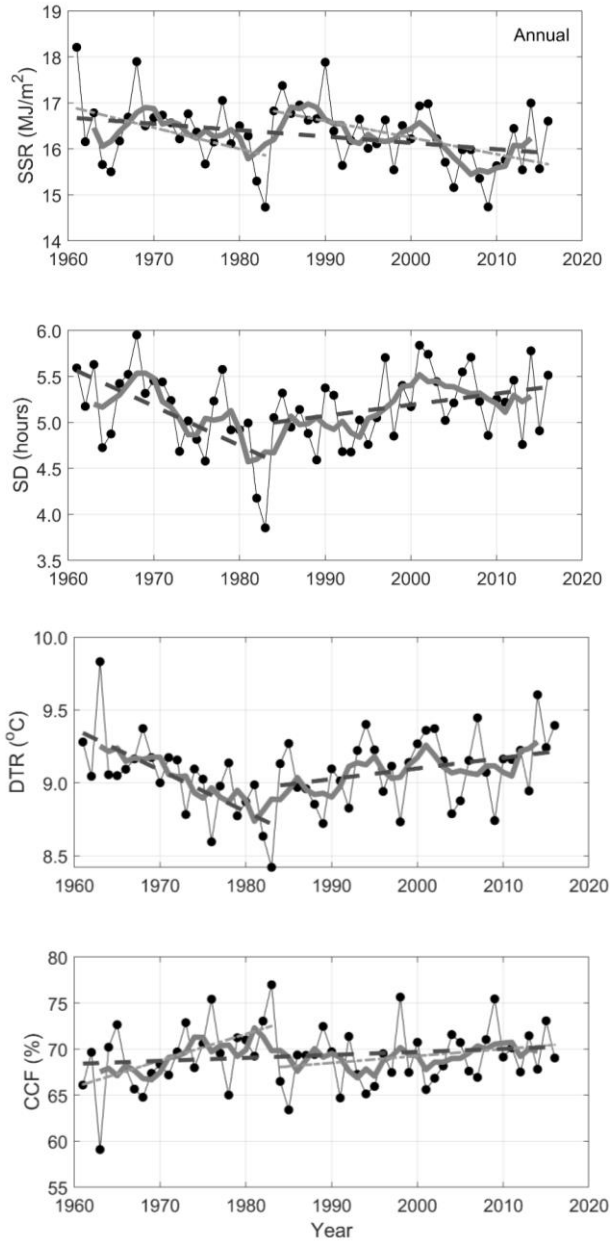
200

201



202

203



204

205

206 Figure 2 – Annual mean variability of surface solar irradiation (SSR), sunshine duration
 207 (SD), diurnal temperature range (DTR) and cloud cover fraction (CCF). Gray curves
 208 represent 5 years moving averages and dotted lines are the result of a trend analysis

209 from 1961 to 1983 and from 1984 to 2016. Lines of the trend analysis for SSR and CCF
210 considering all the analysed years, from 1961 to 2016 are also shown.

211

212 Returning to Fig. 2, the gray curve represents the 5 years moving average, while
213 the dotted lines indicates the result of the modified Mann-Kendall trend analysis,
214 discussed ahead. The year of 1983 was the one presenting the lowest annual mean value
215 for SSR, SD and DTR, clearly as a response to the peak of CCF observed in that year,
216 which is worth to mention, was characterized by a strong El Niño event. According to
217 the Earth System Research Laboratory from the National Oceanic and Atmospheric
218 Administration (ESRL/NOAA), it is listed at the top amongst the 24 strongest El Niño
219 events, in the period from 1895 to 2015, and lasted from April 1982 up to September
220 1983 (<https://www.esrl.noaa.gov/psd/enso/climaterisks/years/top24enso.html>). This
221 1983 El Niño effect was also detected in rainfall data over the São Paulo Metropolitan
222 Area (Obregón et al., 2014), although the authors claim that such influence, at least on
223 rainfall variability, is detectable but is multifaceted and depends on the life cycle of
224 each ENSO event. Xavier et al. (1995), trying to identify a possible influence of ENSO
225 on precipitation extremes in the month of May, classified both May 1983 and May 1987
226 as exceptional extremes of precipitation. Their conclusion was that strong El Niño
227 events can affect the spatial organization of rainfall around São Paulo city. A more
228 recent study performed by Coelho et al. (2017), using daily precipitation data from 1934
229 to 2013 from the same meteorological station analysed in this research, concluded that
230 El Niño conditions in July tend to increase precipitation in the following spring, also
231 anticipating the onset of the rainy season. No study was found about the possible effect
232 of ENSO on cloud cover over São Paulo. According to Rosas et al. (2019), middle and
233 high-level clouds presented high positive anomalous cloud amount in 1983.

234 Applying the piecewise linear regression model (Muggeo, 2003) to detect trend
235 changes, for the variables in Fig. 2, only SD and DTR presented statistically significant
236 breakpoints. For SD, the regime shift was detected in 1982 (± 4 years) ($p = 0.008$) and
237 for DTR, in 1979 (± 4 years) ($p = 0.017$). Considering the uncertainties in the estimates,
238 both include the year 1983, consistent with the findings of Reid et al. (2016), who
239 observed a regime shift in land surface temperature in South America in 1984.~~After~~
240 ~~1983, the trend behaviour of some variables changed, consistent with the findings of~~
241 ~~Reid et al. (2016), who observed a regime shift in land surface temperature in South~~
242 ~~America in 1984.~~ These finding results motivated us to separate the time series
243 analysis in two periods, the first from 1961 to 1983 and the second from 1984 up to
244 2016. The results of the modified Mann-Kendall trend test for each period and for all
245 the analysed years, from 1961 to 2016, are presented in Table 1, considering both
246 annual and seasonal variabilities. Bold values indicate trends that are statistically
247 significant at the 95% confidence level. From the table, in the first period, SSR, SD and
248 DTR presented a decreasing trend, while CCF a positive one, ~~increasing at a rate of~~
249 ~~2.9% per decade~~. Except for SSR, all trends were statistically significant, with daily SD
250 decreasing at a rate of 0.37 hours per decade and the diurnal temperature range
251 declining at a rate of 0.49 °C per decade. As detected by the piecewise linear regression
252 model, SD and DTR changed from negative to positive trends, from the first to the
253 second period. Looking at the seasonal variability, southern hemisphere autumn
254 (MAM), winter (JJA) and springtime (SON) presented statistically significant
255 decreasing trends for SD and DTR. For CCF, statistically significant positive trends
256 were observed for JJA and SON and only MAM presented statistically significant
257 positive trend for SSR in the first period. Considering the whole analysed period, only
258 SSR presented statistically significant trend in the annual basis of $-0.13 \text{ kJm}^{-2} \text{ per}$

Formatado: Não Realce

Formatado: Não Realce

Formatado: Não Realce

Formatado: Não Realce

Formatado: Não Realce

Formatado: Não Realce

Formatado: Não Realce

259 decade. In DJF and MAM the trends were also negative and statistically significant,
 260 while no trends were detected in JJA nor SON. For CCF, a statistically significant trend
 261 change was observed only in MAM of almost 1% per decade. For the other seasons and
 262 in the annual basis, CCF presented no trend (DJF) or positive trend, but not statistically
 263 significant.

Formatado: Não Realce
 Formatado: Não Realce
 Formatado: Não Realce

265 Table 1 - Modified Mann-Kendall trend test results for period 1, from 1961 to 1983, ~~and~~
 266 period 2, from 1984 to 2016, and for all the analysed years, from 1961 to 2016,
 267 considering each season and ~~in~~ on an annual basis for the surface solar radiation (SSR),
 268 sunshine duration (SD), diurnal temperature range (DTR) and sky cover fraction (CCF).
 269 The trend was estimated as the slope of the linear fit between the variable of interest and
 270 year.

SSR									
	1961-1983			1984-2016			1961-2016		
Time interval	Trend^a	Z	p	Trend^a	Z	p	Trend^a	Z	p
Annual	<u>-0.40</u>	<u>-1.64</u>	<u>0.101</u>	<u>-0.39</u>	<u>-3.02</u>	<u>0.003</u>	<u>-0.13</u>	<u>-2.73</u>	<u>0.006</u>
DJF	<u>-0.64</u>	<u>-1.05</u>	<u>0.291</u>	<u>-0.53</u>	<u>-2.56</u>	<u>0.010</u>	<u>-0.26</u>	<u>-2.94</u>	<u>0.003</u>
MAM	<u>-0.76</u>	<u>-2.48</u>	<u>0.013</u>	<u>-0.25</u>	<u>-1.66</u>	<u>0.097</u>	<u>-0.24</u>	<u>-3.14</u>	<u>0.002</u>
JJA	<u>-0.47</u>	<u>-1.93</u>	<u>0.054</u>	<u>-0.17</u>	<u>-1.87</u>	<u>0.061</u>	<u>0.00</u>	<u>-0.16</u>	<u>0.871</u>
SON	<u>-0.24</u>	<u>-0.89</u>	<u>0.373</u>	<u>-0.57</u>	<u>-2.40</u>	<u>0.016</u>	<u>-0.01</u>	<u>-0.74</u>	<u>0.458</u>

SD									
	1961-1983			1984-2016			1961-2016		
Time interval	Trend^b	Z	p	Trend^a	Z	p	Trend^b	Z	p
Annual	<u>-0.37</u>	<u>-3.41</u>	<u>0.001</u>	<u>0.11</u>	<u>2.13</u>	<u>0.033</u>	<u>0.03</u>	<u>0.56</u>	<u>0.577</u>
DJF	<u>-0.41</u>	<u>-1.06</u>	<u>0.291</u>	<u>-0.01</u>	<u>-0.12</u>	<u>0.905</u>	<u>0.02</u>	<u>0.28</u>	<u>0.783</u>
MAM	<u>-0.53</u>	<u>-2.27</u>	<u>0.023</u>	<u>0.22</u>	<u>1.61</u>	<u>0.107</u>	<u>-0.02</u>	<u>-0.19</u>	<u>0.850</u>
JJA	<u>-0.54</u>	<u>-3.38</u>	<u>0.001</u>	<u>0.20</u>	<u>2.06</u>	<u>0.039</u>	<u>0.05</u>	<u>1.17</u>	<u>0.241</u>
SON	<u>-0.47</u>	<u>-2.31</u>	<u>0.021</u>	<u>0.03</u>	<u>0.20</u>	<u>0.840</u>	<u>0.02</u>	<u>0.33</u>	<u>0.745</u>

DTR									
	<u>1961-1983</u>			<u>1984-2016</u>			<u>1961-2016</u>		
<u>Time interval</u>	<u>Trend^c</u>	<u>Z</u>	<u>p</u>	<u>Trend^a</u>	<u>Z</u>	<u>p</u>	<u>Trend^c</u>	<u>Z</u>	<u>p</u>
Annual	-0.49	-3.33	0.001	0.16	1.84	0.065	0.04	0.80	0.425
DJF	-0.32	-1.61	0.107	0.15	1.72	0.085	0.11	3.94	8x10⁻⁵
MAM	-0.58	-2.54	0.011	0.16	1.53	0.125	-0.02	-0.64	0.520
JJA	-0.61	-2.91	0.004	0.14	1.38	0.171	0.06	0.81	0.416
SON	-0.58	-2.64	0.008	0.02	0.17	0.865	0.01	0.13	0.893

CCF									
	<u>1961-1983</u>			<u>1984-2016</u>			<u>1961-2016</u>		
<u>Time interval</u>	<u>Trend^c</u>	<u>Z</u>	<u>p</u>	<u>Trend^a</u>	<u>Z</u>	<u>p</u>	<u>Trend^c</u>	<u>Z</u>	<u>p</u>
Annual	2.9	2.48	0.013	0.8	1.78	0.075	0.3	1.29	0.198
DJF	0.5	0.42	0.673	0.3	0.38	0.700	-0.0	-0.05	0.961
MAM	2.9	1.58	0.113	0.6	0.76	0.448	0.9	2.28	0.023
JJA	3.5	2.54	0.011	0.8	0.57	0.566	0.2	-0.31	0.756
SON	3.8	2.12	0.034	1.5	1.22	0.221	0.4	1.35	0.180

SSR						
	<u>Period 1: 1961-1983</u>			<u>Period 2: 1984-2016</u>		
<u>Time interval</u>	<u>Trend^a</u>	<u>Z</u>	<u>p</u>	<u>Trend^a</u>	<u>Z</u>	<u>p</u>
Annual	-0.40	-1.64	0.101	-0.39	-3.02	0.003
DJF	-0.64	-1.05	0.291	-0.53	-2.56	0.010
MAM	-0.76	-2.48	0.013	-0.25	-1.66	0.097
JJA	-0.47	-1.93	0.054	-0.17	-1.87	0.061
SON	-0.24	-0.89	0.373	-0.57	-2.40	0.016

SD						
	<u>Period 1: 1961-1983</u>			<u>Period 2: 1984-2016</u>		
<u>Time interval</u>	<u>Trend^b</u>	<u>Z</u>	<u>p</u>	<u>Trend^b</u>	<u>Z</u>	<u>p</u>
Annual	-0.37	-3.41	0.001	-0.11	-2.13	0.033

DJF	-0.41	-1.06	0.291	-0.01	-0.12	0.905
MAM	-0.53	-2.27	0.023	-0.22	-1.61	0.107
JJA	-0.54	-3.38	0.001	-0.20	-2.06	0.039
SON	-0.47	-2.31	0.021	-0.03	-0.20	0.840
DTR						
Period 1: 1961-1983			Period 2: 1984-2016			
Time interval	Trend^e	Z	p	Trend^e	Z	p
Annual	-0.49	-3.33	0.001	0.16	1.84	0.065
DJF	-0.32	-1.61	0.107	0.15	1.72	0.085
MAM	-0.58	-2.54	0.011	0.16	1.53	0.125
JJA	-0.61	-2.91	0.004	0.14	1.38	0.171
SON	-0.58	-2.64	0.008	0.02	0.17	0.865
CCF						
Period 1: 1961-1983			Period 2: 1984-2016			
Time interval	Trend^d	Z	p	Trend^d	Z	p
Annual	2.9	2.48	0.013	-0.8	1.78	0.075
DJF	0.5	0.42	0.673	-0.3	0.38	0.700
MAM	2.9	1.58	0.113	-0.6	0.76	0.448
JJA	3.5	2.54	0.011	-0.8	0.57	0.566
SON	3.8	2.12	0.034	-1.5	1.22	0.221

271 Units of trends: a) kJ m^{-2} per decade; b) hours per decade; c) $^{\circ}\text{C}$ per decade; d)

272 % per decade

273 In the first period, SSR and its proxies presented trends consistent with CCF
274 features, i.e., as CCF increased over time, the others decreased. In the second period,
275 from 1984 to 2016, this behaviour combination changed. While SSR still presented, on
276 an annual basis, a statistically significant decreasing trend, of -0.39 kJm^{-2} per decade,
277 SD and DTR trends changed from negative to positive, being statistically significant
278 only for SD, with a trend of 0.11 hours per decade. CCF continued to present a positive

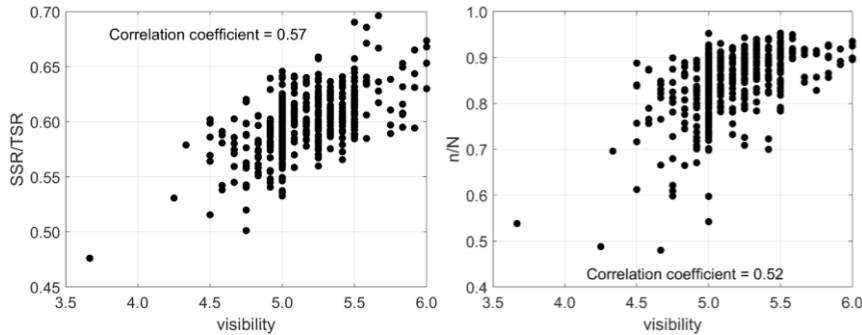
279 trend, but not statistically significant. It is worth noting that, even though the trends are
280 not statistically significant, the pattern between SSR and CCF observed in the first
281 period remained in the second, and in all seasons. According to Rosas et al. (2019),
282 statistically significant trends, positive for low clouds (3.2 % per decade) and negative
283 for mid-level clouds (-5.5 % per decade), were observed in the last 30 years, from 1987
284 to 2016. Such analysis indicated that changes in cloud types also influenced the
285 variability of SSR and proxies. However, other factors, rather than only cloud cover
286 changes, were also responsible for the variability of SD and DTR, as evaluated in the
287 next sections.

288

289 **3.2 Long-term variability of horizontal visibility and of the number of foggy days**

290 To verify how effectively the horizontal visibility acts as a proxy for aerosol
291 optical depth, Fig. 3 shows the solar transmittance (SSR/TSR) and the normalized
292 sunshine duration (n/N) for clear sky days, from July to October, as a function of daily
293 mean visibility. The correlation coefficients are 0.57 and 0.52 for (SSR/TSR) and (n/N),
294 respectively, as indicated in the figure, and for this reason, the visibility data will be
295 analysed next as a proxy for aerosol optical depth. As mentioned in the methodology
296 section, we excluded visibility data from early morning and late afternoon to minimize
297 the influence of fog.

298



299

300 Figure 3 – Daily solar transmittance and the normalized sunshine duration as functions
 301 of the mean horizontal visibility recorded from 10:00 AM to 03:00 PM on clear sky
 302 days in the months of July to October.

303

304 Figure 4 presents the mean visibility from July to October and registered
 305 between 10:00 AM to 03:00 PM, and the number of foggy days in the same months,
 306 from 1961 to 2016, both for all sky conditions. July to October are the months with
 307 lower cloud cover fraction and with higher probability of long-range transport of
 308 biomass burning aerosol particles towards São Paulo, contributing to higher aerosol
 309 optical depth in the city (Castanho and Artaxo, 2001, Landulfo et al., 2003, Freitas et
 310 al., 2005, Castanho et al., 2008, Yamasoe et al., 2017). Since clear sky days are rare in
 311 São Paulo, here we discuss the long-term variability of visibility, trying to infer aerosol
 312 loading variations.

313 From the figure, we see that the highest visibility was observed during the first
 314 half of the 1960's, with a gradual degradation till the early 1970's. ~~From that~~ Thereafter,
 315 visibility increased again but never recovered to the values of the 1960's. A significant
 316 reduction in visibility was observed in 1963. One hypothesis for the lower visibility in
 317 1963 worth investigating was a sequence of vegetation fires reported in August and

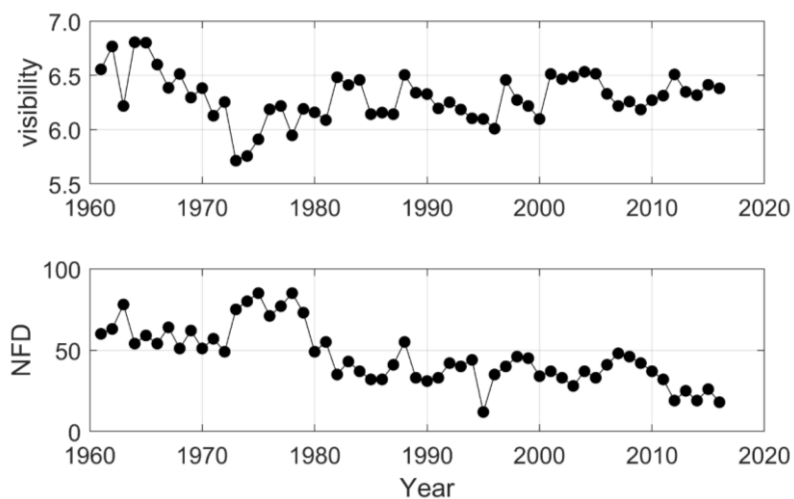
318 September in the state of Paraná affecting 128 municipalities (Paixão and Priori, 2015).
319 Soares (1994) stated that about 10 % of Paraná state was affected by the fires, being
320 responsible for the beginning of fire monitoring in Brazil due to its large proportion.
321 Paraná is located to the south-southwest of the São Paulo state. Cold front systems
322 frequently advect air masses from this region towards São Paulo.

323 Considering local pollution sources, the reduction of the visibility data at the
324 beginning of the series could be associated with the industrialization process in São
325 Paulo, and with the vehicular fleet and changes in the fuel composition, at the end.
326 According to Silva (2011), during 1956 to 1961, a national development plan was
327 implemented in Brazil, to enhance the economic growth, which benefited particularly
328 the city of São Paulo, attracting industries, mainly from the automobile sector. This
329 contributed to increasing the city's population and to the concentration of industries,
330 boosting the economy of São Paulo city. In the 1970's, the high rate of urbanization,
331 with many traffic jams, caused air quality and environmental degradations (Silva,
332 2011). As one of the consequences, the federal government promoted incentives to
333 move industries to other Brazilian states, especially in the north and northeast regions of
334 the country, but a part remained in the Metropolitan Area of São Paulo. Still according
335 to the author, this industrial decentralization process lasted till around 1991.

336 Andrade et al. (2017), discussing changes over time in air quality conditions in
337 the Metropolitan Area of São Paulo, showed that SO₂ frequently exceeded the air
338 quality standards in the 1970's and 1980's. According to the authors, the Brazilian
339 government started a program to control its emissions s due to the complaints of the
340 population. At the beginning, the program focused on stationary sources (industries)
341 and, in the 1990's, the sulfur content in diesel fuel was also targeted. Nonetheless,
342 during that decade, the Metropolitan Area of São Paulo still experienced severe air

343 pollution problems with increasing concentration of aerosol particles, which might
344 explain the reduction in visibility at the beginning of the decade (Fig. 4). Over time,
345 SO₂ emission control and other measures helped decreasing the concentration of SO₂
346 and of particulate matter with diameter less than 10 µm (PM10) near the surface.
347 However, according to Oyama (2015), also due to a political decision to stimulate the
348 economy, the annual number of registrations of new gasoline fuelled vehicles increased
349 exponentially, from about 3000 vehicles in 1988, peaking in 2000 with 150000
350 registrations, and decreasing slowly after that, to about 60000 in 2012. Despite the
351 efforts to reduce vehicular emission, the concentration of particulate matter with
352 diameter less or equal 2.5 µm is not yet controlled. In the recent years, vehicular
353 emission is the main local source of air pollution in the Metropolitan Area of São Paulo
354 (Andrade et al., 2017).

355



356

357 Figure 4 – Time series of the mean visibility recorded from 10:00 AM to 03:00 PM and
358 the number of foggy days (NFD) per year in all sky conditions. Data are limited to the
359 months of July to October.

360

361 Since both SSR and SD presented positive correlation with visibility, another
362 factor might be responsible for the opposite trends observed in the second period for
363 those variables. Changes in the number of foggy days are explored to verify if its
364 variability can help to explain part of the variability observed in the SD trends,
365 particularly after 1983, when CCF only could not explain it. As shown in Fig. 4, the
366 number of days with fog, in the months of July to October each year, is decreasing in
367 São Paulo. The highest numbers were observed during the 1970's with a sharp decrease
368 in the end of the decade and the beginning of the next, followed by a long period of
369 stable conditions up to 2011 when another decrease was observed. This could be the
370 reason for the positive trend of SD under all sky scenarios in the second period (Fig. 2),
371 when the CCF increase was not significant. A decrease in the annual number of foggy
372 days was also observed in China (Li et al., 2012), which the authors attributed to the
373 urban heat island effect. São Paulo, throughout the analysed period in this study,
374 experienced a significant change in its spatial domain, which contributed to the
375 intensification of the urban heat island effect. More on this effect will be discussed in
376 the next section.

377

378 **3.3 Long term trends in daily maximum and minimum temperatures**

379 Figure 5 presents the temporal variation of the annual mean of the daily
380 maximum and minimum temperatures registered at the meteorological station, used to

381 estimate DTR. As discussed in the last section, if the increasing trend in SD over the
382 last years could be possibly attributed to the decreasing number of days per year with
383 fog occurrence, we now hypothesize on the possible reasons for the increasing trend of
384 DTR in the second period. According to Dai et al. (1999), DTR should also respond to
385 cloud cover and precipitation and thus to SSR variations. As discussed by the authors,
386 clouds can reduce T_{max} and increase T_{min} , since they can reflect solar radiation back to
387 space during daytime and emit thermal radiation down to the surface during the night,
388 respectively. Such behaviours can be clearly seen in Fig. 5, in the first period, and
389 confirmed by the trend analysis presented in Table 2. During the dimming period, T_{max}
390 presented a negative trend, while T_{min} an increasing one, statistically significant at 95 %
391 confidence level for the ~~latterst~~ variable. SA similar behaviour was observed by Wild et
392 al. (2007) who argued that the decreasing trend of T_{max} is consistent with the negative
393 trend of SSR, demonstrating that solar radiation deficit at the surface presented a clear
394 effect on the surface temperature. Looking at the second period, from 1984 to 2016,
395 both maximum and minimum temperatures presented increasing trends, statistically
396 significant at the 95 % confidence level, ~~on an~~ⁱⁿ the annual basis, of 0.25 °C per decade
397 and 0.16 °C per decade, respectively. In this period, ~~the~~ T_{min} trend was still in line with
398 the increasing CCF trend, but as pointed out by Wild et al. (2007) it could also be a
399 response to the increasing levels of greenhouse gases as also pointed ~~out~~ by de Abreu et
400 al. (2019) for the south-eastern part of Brazil where São Paulo is located. Like SSR and
401 CCF, these variables presented no statistically significant regime shift when applying
402 the piecewise regression model. Thus, considering the whole period, it is possible to
403 observe that regardless of the season or in the annual basis, both T_{max} and T_{min} presented
404 statistically significant positive trends. T_{max} increased with a trend of about 0.30 °C per

Formatado: Não Realce

Formatado: Não Realce

decade and T_{\min} at a rate of 0.25 °C per decade, being the highest trend detected in the summer months of DJF.

Table 2 - Modified Mann-Kendall trend test results for period 1, from 1961 to 1983, period 2, from 1984 to 2016, and all the analysed years, from 1961 to 2016, considering each season and in an annual basis, for the daily maximum (T_{\max}) and minimum (T_{\min}) temperatures. The trend was estimated as the slope of the linear fit between the variable of interest and year.

Tmax									
	1961-1983			1984-2016			1961-2016		
Time interval	Trend	Z	p	Trend	Z	p	Trend	Z	p
Annual	-0.11	-1.33	0.184	0.25	2.15	0.031	0.30	4.69	<10⁻⁵
DJF	0.20	1.06	0.291	0.33	2.07	0.038	0.42	4.91	<10⁻⁶
MAM	-0.15	-0.79	0.430	0.03	0.23	0.816	0.22	3.25	0.001
JJA	0.02	0.26	0.795	0.33	2.68	0.007	0.23	3.17	0.023
SON	-0.26	-0.63	0.526	0.36	1.72	0.085	0.32	3.23	0.001

Tmin									
	1961-1983			1984-2016			1961-2016		
Time interval	Trend	Z	p	Trend	Z	p	Trend	Z	p
Annual	0.56	2.54	0.011	0.16	2.15	0.031	0.25	5.68	<10⁻⁷
DJF	0.53	2.96	0.003	0.13	2.68	0.007	0.31	5.66	<10⁻⁷
MAM	0.52	2.71	0.007	-0.07	-0.79	0.429	0.27	3.17	0.002
JJA	0.62	1.58	0.113	0.26	1.78	0.075	0.18	2.66	0.008
SON	-0.03	0.63	0.526	0.26	2.43	0.015	0.27	6.68	<10⁻⁹

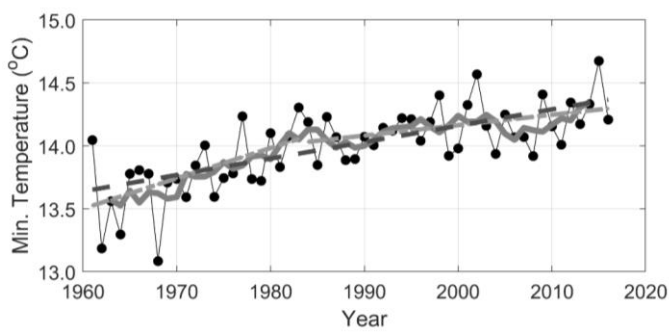
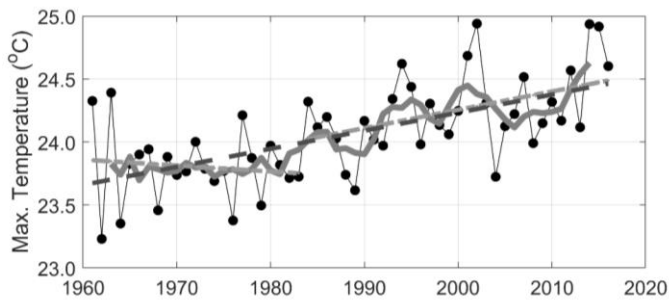
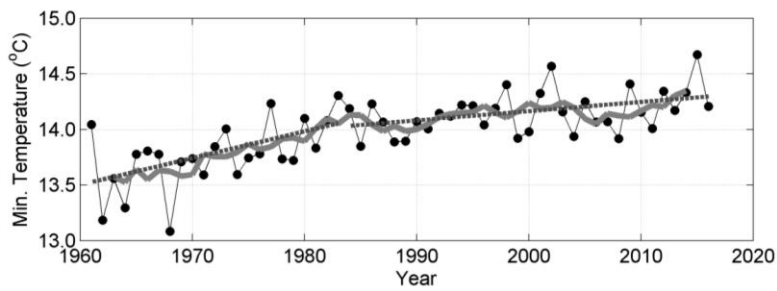
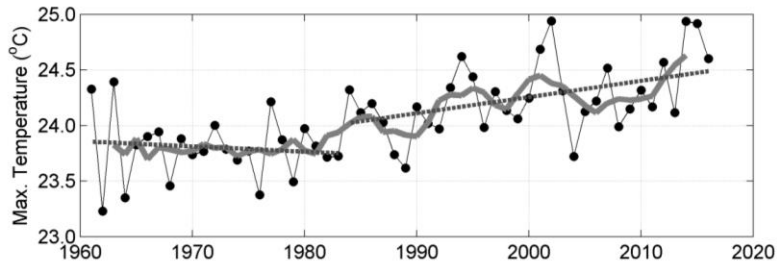
Table 2—Modified Mann-Kendall trend test results for period 1, from 1961 to 1983, and period 2, from 1984 to 2016, considering each season and in an annual basis, for the daily maximum (T_{\max}) and minimum (T_{\min}) temperatures. The trend was estimated as the slope of the linear fit between the variable of interest and year.

T_{max}						
	Period 1: 1961-1983			Period 2: 1984-2016		
Time interval	Trend	Z	p	Trend	Z	p
Annual	-0.11	-1.33	0.184	0.25	2.15	0.031
DJF	-0.20	-1.06	0.291	0.33	2.07	0.038
MAM	-0.15	-0.79	0.430	0.03	0.23	0.816
JJA	-0.02	-0.26	0.795	0.33	2.68	0.007
SON	-0.26	-0.63	0.526	0.36	1.72	0.085

T_{min}						
	Period 1: 1961-1983			Period 2: 1984-2016		
Time interval	Trend	Z	p	Trend	Z	p
Annual	0.56	2.54	0.011	0.16	2.15	0.031
DJF	0.53	2.96	0.003	0.13	2.68	0.007
MAM	0.52	2.71	0.007	-0.07	-0.79	0.429
JJA	0.62	1.58	0.113	0.26	1.78	0.075
SON	-0.03	0.63	0.526	0.26	2.43	0.015

418 Units of trend: °C per decade

419



420

421

422 Figure 5 - Annual mean variability of daily maximum and minimum air temperatures at
 423 1.5 meters. Gray curves represent 5 years moving averages, light-gray-dotted lines are
 424 the result of trend analysis from 1961 to 1983 and from 1984 to 2016 and the dark-gray-

425 ~~dotted line represents the trend from 1961 to 2016 and dotted lines are the result of trend~~
426 ~~analysis from 1961 to 1983 and from 1984 to 2016.~~

427
428 The urban heat island (UHI) effect could also be responsible ~~to~~for the observed
429 increasing trend of T_{\max} , particularly after 1980. The Metropolitan Area of São Paulo
430 experienced a fast growth rate from 1980 to 2010. There were nearly 12 million
431 inhabitants in 1980, and the population grew to about 21 million inhabitants in 2010
432 (Silva et al., 2017). According to the authors, the urban area increased from 874 km² to
433 2209 km², from 1962 to 2002. According to Kim and Baik (2002), the maximum UHI
434 intensity is more pronounced in clear sky conditions, occurs more frequently at night
435 than during the day, and decreases with increasing wind speed. However, Ferreira et al.
436 (2012) reported that, in São Paulo, the urban heat island maximum effect was observed
437 during daytime, around 03:00 PM, and was associated with downward solar radiation
438 heating the urban region in a more effective way than the rural surrounding areas.

439 Finally, as pointed out by Wild et al. (2007), the increasing atmospheric
440 concentration of greenhouse gases (GHG) can be another reason for the observed trend
441 of T_{\max} , which was masked by the dimming effect in the first period. Modelling studies
442 can help verify the real causes and disentangle the contribution of each effect, which is,
443 however, out of the scope of this work.

445 **4 Conclusions**

446 This analysis of 56 years of surface solar irradiation (SSR) and proxies (SD and
447 DTR) data helped to show that from about 1960 to the early 1980s, named as first
448 period, a dimming effect of surface solar radiation was observed in the city of São
449 Paulo, consistent ~~to~~with other parts of the world. The positive trend of CCF in the first

450 period indicates that cloud ~~variability-cover changes~~ could be one important driver of
451 the dimming period. The dimming effect was also confirmed by SD and DTR trends in
452 the mentioned period. However, the consistency between SSR, SD and DTR trends
453 ended ~~in-around~~ 1983, when CCF presented the highest value throughout the entire
454 series and which coincided with a strong El Niño year. Thus, answering our first
455 question, SSR presented a decreasing trend, throughout the 56 years of data, ~~statistically~~
456 ~~significant at the 95% confidence level, with a rate of -0.13 kJ m^{-2} per decade. The~~
457 ~~negative trend was statistically significant also in DJF and MAM, presenting the most~~
458 ~~negative trend in the summer (DJF) of -0.26 kJ m^{-2} per decade, though not statistically~~
459 ~~significant at the 95% confidence level in the first period, while it decreased at a rate of~~
460 ~~-0.39 kJ m^{-2} per decade in the second one, from 1984 to 2016.~~

461 ~~Applying a piecewise linear regression model to the variables, only SD and DTR~~
462 ~~presented a statistically significant regime shift, around 1982 and 1979, respectively,~~
463 ~~with uncertainty of four years in both results. As the negative SSR trend was consistent~~
464 ~~with the slight positive trend of CCF, the changing behaviour of SD and DTR indicated~~
465 ~~that other factors besides the cloud cover variability might have affected their distinct~~
466 ~~patterns. In the second period, the negative SSR trend was still consistent with the slight~~
467 ~~positive trend of CCF, while the opposite behaviour of SD and DTR indicated that other~~
468 ~~factors besides the cloud cover variability might have affected their distinct patterns. In~~
469 order to understand the possible causes of the SD trends, alternative parameters (fog
470 frequency and horizontal visibility) focusing on the dry months of July to October, were
471 analysed. The results indicated that the decreasing trend of the number of foggy days
472 per year ~~may~~ explains part of the increasing trend of SD.

473 Moreover, on clear sky days, both SSR and SD presented correlation coefficients
474 above 0.5 with visibility for the period when fog is unlikely to occur, indicating that this

Formatado: Não Realce

475 variable could be used as a proxy for aerosol loading variations. Changes in visibility
476 during the 1960s and 1970s could be associated ~~to~~with the dynamics of the
477 industrialization process of São Paulo Metropolitan Area and the consequent
478 urbanization, with population growth, traffic jams and the degradation of the air quality.
479 Long-range transport of biomass burning products towards São Paulo is also an
480 important source of aerosol during the dry season. However, the long-term contribution
481 of the different regions, as sources of pollutants to the atmosphere of the Metropolitan
482 Area of São Paulo is unclear. The role of biomass burning, in the state of São Paulo and
483 the neighbour states of Minas Gerais, Paraná and Mato Grosso, is yet to be clarified.
484 Further research is needed to improve our historical perspective on the role of other
485 regional air pollution sources on the SSR.

486 In the case of DTR, since it was obtained from the difference between the daily
487 maximum and minimum air temperatures close to the surface, the trends of the annual
488 mean values of these temperatures were separately determined and analysed. The T_{\min}
489 positive trends followed the CCF ones, with also a possible influence of the increasing
490 levels of greenhouse gases, noticing that the reduction observed in CCF, in the
491 beginning of the second period, is absent in the T_{\min} time series. The increasing trend of
492 CCF, in the first period, resulted in a decreasing trend in T_{\max} , as more solar radiation
493 reaching the surface was attenuated from year to year due to the presence of clouds.
494 Some hypotheses for the increasing trend of T_{\max} during the second period were the
495 urban heat island effect and the increasing concentrations of GHG. Of course, changes
496 in the wind pattern and consequently in the advection of air masses with distinct
497 properties can also affect the air temperature locally.

498 As the resultant trends of SD and DTR, compared with the SSR trend, diverged
499 in the second period for São Paulo, in all sky conditions, caution might be taken when

500 those variables are used as proxies to downward surface solar radiation in the context of
501 dimming and brightening analyses. This study revealed that different factors may act on
502 each variable, leading to a distinct behaviour, as also mentioned by Manara et al.
503 (2017).

504 For future studies, modelling efforts may be able to help evaluate each
505 hypothesis raised in the present study, either those related to climate natural variability,
506 such as El Niño, or ~~to~~ those arising from anthropogenic activities as the increase of
507 greenhouse gas concentrations, land use changes, particularly through the
508 imperviousness of soils, affecting the partitioning of latent and sensible heat fluxes.
509 Also, a higher temporal analysis and simultaneous monitoring of aerosol optical
510 properties will help to better evaluate the aerosol effect on downward solar radiation in
511 this region, including via the indirect effect.

512

513 **Data availability**

514 Access to IAG meteorological station database (sky cover fraction, sunshine duration,
515 daily maximum and mi~~n~~imum air temperatures, number of foggy days, visibility and
516 irradiation data) for education or scientific use can be made under request at
517 http://www.estacao.iag.usp.br/sol_dados.php. All processed data used in the manuscript
518 such as annual and seasonal mean values, as well as data from cloud free days can be
519 found at <https://www.iag.usp.br/lraa/index.php/data/cientec/weather-station-climatology/>.

521

522 **Author contribution**

523 Conceptualization MAY and NMER; Methodology MAY; Data organization MAY and
524 SNSMA; Formal analysis MAY; Writing original draft MAY and NMER; Writing –
525 Review & Editing MAY, NMER, MW.

526

527 **Competing interest**

528 The authors declare that they have no conflict of interest.

529

530 **Acknowledgements**

Formatado: Português (Brasil)

531 The authors acknowledge Fundação de Amparo à Pesquisa do Estado de São Paulo
532 (FAPESP), grant number 2018/16048-6 and Coordenação de Aperfeiçoamento de
533 Pessoal de Nível Superior (CAPES) for financial support. Yamasoe acknowledges
534 CNPq (Conselho Nacional de Desenvolvimento Científico e Tecnológico), process
535 number 313005/2018-4. [Global dimming and brightening research at ETH Zurich is](#)

536 [funded by the Swiss National Science Foundation \(Grant number 200020 188601\).](#) This

Formatado: Português (Brasil)

537 study is part of the Núcleo de Apoio à Pesquisa em Mudanças Climáticas (INCLINE)

538 [and of Processos Radiativos na Atmosfera – Impactos dos Gases, Aerossóis e Nuvens.](#)

Formatado: Português (Brasil)

539 The authors are grateful to the observers and staff of the Instituto de Astronomia,
540 Geofísica e Ciências Atmosféricas meteorological station for making available the
541 meteorological observations. [The authors acknowledge the two anonymous referees for](#)
542 [their time, comments and suggestions that helped improve and clarify this paper.](#)

543

544 **References**

545 Andrade, M. F., Kumar, P., Freitas, E. D., Ynoue, R. Y., Martins, J., Martins, L. D.,
546 Nogueira, T., Perez-Martinez, P., Miranda, R. M., Albuquerque, T., Gonçalves, F. L. T.,
547 Oyama, B. and Zhang, Y. Air quality in the megacity of São Paulo: Evolution over the
548 last 30 years and future perspectives. *Atmospheric Environment* 159, 66-82, 2017.

549 Bristow, K. L. and Campbell, G. S. On the relationship between incoming solar
550 radiation and daily maximum and minimum temperature. *Agricultural and Forest*
551 *Meteorology* 31, 159-166, 1984.

552 Castanho, A. D. A. and Artaxo, P. Wintertime and summertime São Paulo aerosol
553 source apportionment study. *Atmospheric Environment* 35, 4889-4902, 2001.

554 Castanho, A. D. de A., Martins, J. V. and Artaxo, P. MODIS aerosol optical depth
555 retrievals with high spatial resolution over an urban area using the critical reflectance. *J.*
556 *Geophys. Res.* 113, D02201, doi: 10.1029/2007JD008751, 2008.

557 Coelho, C. A. S., Firpo, M. A. F., Maia, A. H. N., and MacLachlan, C. Exploring the
558 feasibility of empirical, dynamical and combined probabilistic rainy season onset
559 forecasts for São Paulo, Brazil. *Int. J. Climatol.* 37 (Suppl. 1), 398-411, doi:
560 10.1002/joc.5010, 2017.

561 Dai, A., Trenberth, K. E. and Karl, T. R. Effects of clouds, soil moisture, precipitation,
562 and water vapor on diurnal temperature range. *Journal of Climate* 12, 2451-2473, 1999.

563 de Abreu, R. C., Tett, S. F. B., Schurer, A. and Rocha, H. R. Attribution of detected
564 temperature trends in Southeast Brazil. *Geophysical Research Letters*, 46, 8407-8414.
565 <https://doi.org/10.1029/2019GL083003>, 2019.

566 Dutton, E. G., Stone, R. S., Nelson, D. W. and Mendonca, B. G. Recent interannual
567 variations in solar radiation, cloudiness, and surface temperature at the South Pole.
568 *Journal of Climate* 4, 848-858, 1991.

569 Ferreira, M. J., Oliveira, A. P., Soares, J., Codato, G., Bárbaro, E. W. and Escobedo, J.
570 F. Radiation balance at the surface in the city of São Paulo, Brazil: diurnal and seasonal
571 variations. *Theor. Appl. Climatol.* 107-229-246. doi: 10.1007/s00704-011-0480-2,
572 2012.

573 Freitas, S. R., K. M. Longo, M. A. F. S. Dias, P. L. S. Dias, R. Chatfield, E. Prins, P.
574 Artaxo, G. A. Grell, and F. S. Recuero. Monitoring the transport of biomass burning
575 emissions in South America, *Environ. Fluid Mech.*, 5, 135-167, 2005.

576 Hamed, K. H. and Rao, A. R. A modified Mann-Kendall trend test for autocorrelated
577 data. *Journal of Hydrology* 204, 182-196, 1998.

578 Horseman, A., MacKenzie, A. R. and Timmis, R. Using bright sunshine at low-
579 elevation angles to compile an historical record of the effect of aerosol on incoming
580 solar radiation. *Atmos. Environ.* 42, 7600-7610, 2008.

581 Kazadzis, S., Founda, D., Psiloglou, B. E., Kambezidis, H., Mihalopoulos, N., Sanchez-
582 Lorenzo, A., Meleti, C., Raptis, P. I., Pierros, F., and Nabat, P. Long-term series and

Formatado: Português (Brasil)

583 trends in surface solar radiation in Athens, Greece, *Atmos. Chem. Phys.*, 18, 2395–
584 2411, <https://doi.org/10.5194/acp-18-2395-2018>, 2018.

585 Kim, Y.H. and Baik J. J. Maximum urban heat island intensity in Seoul. *J. Appl.*
586 *Meteorol.*, 41, 651–659, 2002.

587 Kren, A. C., Pilewskie, P. and Coddington, O. Where does Earth’s atmosphere get its
588 energy? *J. Space Weather Space Clim.* 7(A10) doi: 10.1051/swsc/2017007, 2017.

589 Kumari, B. P. and Goswami, B. N. Seminal role of clouds on solar dimming over India
590 monsoon region. *Geophys. Res. Letters* 37 (L06703), 1-5, doi:10.1029/2009GL042133,
591 2010.

592 Landulfo, E., A. Papayannis, P. Artaxo, A. D. A. Castanho, A. Z. Freitas, R. F. Sousa,
593 N. D. Vieira Jr., M. P. M. P. Jorge, O. R. Sánchez-Ccoyllo, and D. S. Moreira.
594 Synergetic measurements of aerosols over São Paulo, Brazil using LIDAR,
595 Sunphotometer and satellite data during the dry season, *Atmos. Chem. Phys.*, 3, 1523–
596 1539, 2003.

597 Li, Z., Yang, J., Shi, C. and Pu, M. Urbanization effects on fog in China: Field Research
598 and Modeling. *Pure Appl. Geophys.* 169, 927-939, doi: 10.1007/s00024-011-0356-5,
599 2012.

600 Makowski, K., Wild, M. and Ohmura, A. Diurnal temperature range over Europe
601 between 1950 and 2005. *Atmos. Chem. Phys.*, 8, 6483–6498, 2008.

602 Manara, V., Brunetti, M., Celozzi, A., Maugeri, M., Sanchez-Lorenzo, A. and Wild, M.
603 Detection of dimming/brightening in Italy from homogenized all-sky and clear-sky
604 surface solar radiation records and underlying causes (1959-2013). *Atmos. Chem. Phys.*
605 16, 11145-11161, doi:10.5194/acp-16-11145-2016, 2016.

606 Manara, V., Brunetti, M., Maugeri, M., Sanchez-Lorenzo, A. and Wild, M. Sunshine
607 duration and global radiation trends in Italy (1959–2013): To what extent do they agree?
608 *J. Geophys. Res. Atmos.* 122, 4312–4331, doi:10.1002/2016JD026374, 2017.

609 Manara, V., Bassi, M., Brunetti, M. et al. 1990–2016 surface solar radiation variability
610 and trend over the Piedmont region (northwest Italy). *Theor. Appl. Climatol.* 136, 849–
611 862, doi: 10.1007/s00704-018-2521-6, 2019.

612 Muggeo, V. M. R. Estimating regression models with unknown break-points. *Statist.*
613 *Med.* 22, 3055–3071. doi: 10.1002/sim.1545, 2003.

614 Obregón G. O., Marengo J. A. and Nobre C. A. Rainfall and climate variability: long-
615 term trends in the Metropolitan Area of São Paulo in the 20th century. *Clim Res* 61:93-
616 107. <https://doi.org/10.3354/cr01241>, 2014.

617 Ohvriil, H., Teral, R., Neiman, L., Kannel, M., Uustare, M., Tee, M., Russak, V.,
618 Okulov, O., Jõeveer, A., Kallis, A., Ohvriil, T., Terez, E. I., Terez, G. A., Gushchin, G.
619 K., Abakumova, G. M., Gorbarenko, E. V., Tsvetkov, A. V. and Laulainen, N. Global
620 dimming and brightening versus atmospheric column transparency, Europe, 1906-2007.
621 *J. Geophys. Res.* 114(D00D12), 1-17, doi:10.1029/2008JD010644, 2009.

Formatado: Português (Brasil)

Formatado: Não Realce

622 Oyama, B. S. Contribution of the vehicular emission to the organic aerosol composition
623 in the city of São Paulo. (Doctoral Thesis). Universidade de São Paulo, São Paulo,
624 Brazil. Available at
625 https://www.iag.usp.br/pos/sites/default/files/t_beatriz_s_oyama_corrigida.pdf - last
626 access on October 25, 2019, 2015.

627 Paixão, L. A. and Priori, A. A. Social and environmental transformations of the rural
628 landscape after an environmental disaster (Paraná, Brazil, 1963). *Estudos Históricos*
629 28(56), 323-342, <http://dx.doi.org/10.1590/S0103-21862015000200006>, 2015.

630 Paltridge, G. W. and Platt, C. M. R. Radiative processes in meteorology and
631 climatology. Elsevier Science, Amsterdam, Oxford, New York, 1976.

632 Plana-Fattori, A. and Ceballos, J. C. Algumas análises do comportamento de um
633 actinógrafo bimetalico Fuess modelo 58d. *Revista Brasileira de Meteorologia* 3 (2),
634 247-256, 1988.

635 Raichijk, C. Observed trends in sunshine duration over South America. *International*
636 *Journal of Climatology* 32, 669-680. doi: 10.1002/joc.2296, 2012.

637 Reid, P. C., Hari, R. E., Beaugrand, G., Livingstone, D. M., Marty, C., Straile, D.,
638 Barichivich, J., Goberville, E., Adrian, R., Aono, Yasuyuki, Brown, R., Foster, J.
639 Groisman, P., Hélaouët, P., Hsu, H.-H., Kirby, R., Knight, J., Kraberg, A., Li, J., Lo, T.-
640 T., Myneni, R. B., North, R. P., Pounds, J. A., Sparks, T., Stübi, R., Tian, Y., Wiltshire,
641 K. H., Xiao, D. and Zhu, Z. Global impacts of the 1980s regime shift. *Global Change*
642 *Biology* 22, 682-703. doi: 10.1111/gcb.13106, 2016.

643 Rosas, J., Yamasoe, M. A., Sena E. T. and Rosário N. E. Cloud climatology from visual
644 observations at São Paulo, Brazil. *Int. J. Climatol.*, 1-13.
645 <https://doi.org/10.1002/joc.6203>, 2019.

646 Sen, P. K. Estimates of the regression coefficient based on Kendall's Tau. *Journal of the*
647 *American Statistical Association* 63(324), 1379-1389, 1968.

648 Shi, G., Hayasaka, T., Ohmura, A., Chen, Z.-H., Wang, B., Zhao, J.-Q., Che, H.-Z. and
649 Xu, Li. Data quality assessment and the long-term trend of ground solar radiation in
650 China. *Journal of Applied Meteorology and Climatology* 47, 1006-1016, 2008.

651 Silva, F. B., Longo, K. M., and Andrade, F. M. Spatial and temporal variability patterns
652 of the urban heat island in São Paulo. *Environments* 4, 27, doi:
653 10.3390/environments4020027, 2017.

654 Silva, P. F. J. Notas sobre a industrialização no estado de São Paulo, Brasil. *Finisterra*,
655 XLVI 91, 87-98, 2011.

656 Soares, R. V. Ocorrência de incêndios em povoados florestais. *Floresta* 22(1/2), 39-
657 53, 1994.

658 Stanhill, G. and Cohen, S. Global dimming: a review of the evidence for a widespread
659 and significant reduction in global radiation with discussion of its probable causes and

Formatado: Português (Brasil)

Formatado: Português (Brasil)

Formatado: Português (Brasil)

Formatado: Inglês (Reino Unido)

660 possible agricultural consequences. *Agricultural and Forest Meteorology* 107, 255-278,
661 2001.

662 Stanhill, G., Achiman, O., Rosa, R. and Cohen, S. The cause of solar dimming and
663 brightening at the Earth's surface during the last half century: Evidence from
664 measurements of sunshine duration. *J. Geophys. Res. Atmos.* 119, 10902-10911.
665 doi:10.1002/2013JD021308, 2014.

666 Xavier, T. M. B. S., Silva Dias, M. A. F. and Xavier, A. F. S. Impact of ENSO episodes
667 on the autumn rainfall patterns near São Paulo, Brazil. *Int. J. Climatol.* 15, 571-584,
668 1995.

669 Wild, M., Gilgen, H., Roesch, A., Ohmura, A., Long, C. N., Dutton, E. G., Forgan, B.,
670 Kallis, A., Russak, V., and Tsvetkov, A. From dimming to brightening: decadal changes
671 in solar radiation at Earth's surface. *Science* 308, 847-850, 2005.

672 Wild, M., Ohmura, A., and Makowski, K. Impact of global dimming and brightening on
673 global warming. *Geophys. Res. Lett.* 34, L04702, doi: 10.1029/2006GL028031, 2007.

674 Wild, M. Global dimming and brightening: A review. *J. Geophys. Res.* 114(D00D16),
675 doi: 10.1029/2008JD011470, 2009.

676 Wild, M. Enlightening global dimming and brightening. *BAMS* 93, 27-37,
677 doi:10.1175/BAMS-D-11-00074.1, 2012.

678 Wild, M., Folini, D., Schär, C., Loeb, N., Dutton, E. G. and König-Langlo, G. The
679 global energy balance from a surface perspective. *Clim. Dyn.* 40, 3107-3134, doi:
680 10.1007/s00382-012-1569-8, 2013.

681 Wild, M. Towards global estimates of the surface energy budget. *Curr. Clim. Change*
682 *Rep.* 3, 87-97. doi: 10.1007/s40641-017-0058-x, 2017.

683 Yamasoe, M. A., N. M. E. do Rosário, and K. M. Barros. Downward solar global
684 irradiance at the surface in São Paulo city—The climatological effects of aerosol and
685 clouds, *J. Geophys. Res. Atmos.*, 122, 391–404, doi:10.1002/2016JD025585, 2017.

686 Yang, S., Wang, X. L. and Wild, M. Causes of Dimming and Brightening in China
687 Inferred from Homogenized Daily Clear-Sky and All-Sky in situ Surface Solar
688 Radiation Records (1958-2016). *Journal of Climate* 32, 5901-5913, doi: 10.1175/JCLI-
689 D-18-0666.1, 2019.

690 Zerefos, C.S., Eleftheratos, K., Meleti, C., Kazadzis, S., Romanou, A., Ichoku, C.,
691 Tselioudis, G. and Bais, A. Solar dimming and brightening over Thessaloniki, Greece,
692 and Beijing, China. *Tellus B*, 61: 657-665. doi:10.1111/j.1600-0889.2009.00425.x,
693 2009.

694 Zhang, S., W., J., Fan, W., Yang, Q. and Zhao, D. Review of aerosol optical depth
695 retrieval using visibility data. *Earth-Science Reviews* 200, 102986,
696 <https://doi.org/10.1016/j.earscirev.2019.102986>, 2020.

Formatado: Português (Brasil)